



Universiteit  
Leiden  
The Netherlands

## Spin-label EPR on Disordered and Amyloid Proteins

Hashemi Shabestari, M.

### Citation

Hashemi Shabestari, M. (2013, April 16). *Spin-label EPR on Disordered and Amyloid Proteins*. Retrieved from <https://hdl.handle.net/1887/20749>

Version: Not Applicable (or Unknown)

License: [Leiden University Non-exclusive license](#)

Downloaded from: <https://hdl.handle.net/1887/20749>

**Note:** To cite this publication please use the final published version (if applicable).

Cover Page



Universiteit Leiden



The handle <http://hdl.handle.net/1887/20749> holds various files of this Leiden University dissertation.

**Author:** Hashemi Shabestari, Maryam

**Title:** Spin-label EPR on disordered and amyloid proteins

**Issue Date:** 2013-04-16

# **CHAPTER 2**

## **THE EFFECT OF A MEMBRANE MIMICKING DETERGENT ON AMYLOID $\beta$ AGGREGATION**

### ***OVERVIEW AND THE REGIME OF HIGH DETERGENT CONCENTRATION***

The aggregation of amyloid  $\beta$  ( $A\beta$ ) peptide into fibrils and plaques is the chief indicator of Alzheimer's disease. Specific interest in oligomers stems from the suggestion that small, oligomeric aggregates and protofibrils, rather than the fully formed fibrils could be responsible for the toxicity of the  $A\beta$  peptide. We investigate the potential of Electron Paramagnetic Resonance (EPR) spectroscopy to detect early stages of  $A\beta$  peptide aggregation in the presence of the sodium dodecyl sulfate (SDS) detergent as a membrane mimicking agent. We have labeled the  $A\beta_{40}$  peptide variant, which contains an N-terminal cysteine with the MTS spin label ((1-oxyl-2,2,5,5-tetramethylpyrroline-3-methyl) methanethiosulfonate) and monitor the effect of different concentrations of SDS on the aggregation of the  $A\beta$  peptide. Continuous wave, 9 GHz EPR reveals that upon increasing the SDS concentration a transition from oligomers to a state in which a monomeric peptide binds to a micelle occurs. In the hitherto difficult to access area of low SDS concentrations we postulate a change from  $A\beta$  oligomers to  $A\beta$ -SDS complexes. The EPR approach enables us to monitor the changes occurring in the reaction mixture in the presence of different amounts of SDS on the time scale of aggregation.

M. Hashemi Shabestari, N.J. Meeuwenoord, D.V. Filippov, M. Huber.

## 2.1 Introduction

The amyloid  $\beta$  (A $\beta$ ) peptide is important in the context of Alzheimer's disease, where it is one of the major components of the fibrils forming amyloid plaques<sup>[1-6]</sup>. The peptide derives from misprocessing of the amyloid precursor protein (APP) and comprises a part of the presumed transmembrane section of APP<sup>[3,5-9]</sup>. In solution, the peptide is disordered and, especially at high concentration its tendency to aggregate into fibrils is high<sup>[10]</sup>. In the fibrils it adopts a parallel,  $\beta$ -sheet structure<sup>[3,11]</sup>.

In vitro studies of the properties of A $\beta$  are essential to understand its behavior at a molecular level. Such studies should also address the aggregation process, in particular, since early aggregates such as oligomers, rather than fully formed plaques, are discussed as toxic agents<sup>[5,8,12-16]</sup>. Furthermore, agents that can influence aggregation are important, and of those, membrane mimics are particularly relevant, because the hydrophobic part of A $\beta$  suggests a possible membrane activity of the peptide. One such agent is the sodium dodecyl sulfate (SDS) detergent<sup>[17-21]</sup>.

The aggregation of A $\beta$  under the influence of SDS, and with respect to the SDS concentration has identified two regimes<sup>[20]</sup>. At low concentrations of SDS or low SDS to peptide ratios (D/P), evidence for aggregates was found. These aggregates appeared to have a  $\beta$ -sheet component<sup>[22-27]</sup>, suggesting aggregates which possess the secondary structure element of A $\beta$  in the fibrils. In this regime, solution NMR methods are plagued by the absence of signals<sup>[20]</sup>, which together with the known heterogenic character of A $\beta$  samples has precluded further structural characterization. At higher SDS concentrations, the picture becomes clearer. In the concentration range around the critical micelle concentration (CMC) of SDS in water<sup>[22-25,27]</sup> and above, A $\beta$  is found to have an  $\alpha$ -helical conformation. A detailed study, using solution NMR<sup>[20,28]</sup> revealed that A $\beta$  could be monomeric and embedded in an SDS micelle, a model that is supported also by small-angle X-ray and neutron scattering, FTIR, and CD spectroscopy<sup>[16,17,20,28-34]</sup>.

In the present study, we use spin-label EPR to learn more about the aggregation process in the presence of SDS. There are several reports about the use of spin-label EPR in A $\beta$  research<sup>[35-37]</sup>. The most relevant in the present context is that signatures of the oligomeric A $\beta$  peptide can be detected by the spin-label EPR methodology<sup>[38]</sup>, suggesting this technique as a possible tool to detect the effect of SDS on the aggregation of A $\beta$  peptide. We employ spin-label EPR in combination with diamagnetic dilution to avoid line broadening by spin-spin interactions<sup>[3,38,39]</sup>. Diamagnetic dilution refers to diluting the spin-labeled A $\beta$  peptide (SL-A $\beta$ ) with

unlabeled A $\beta$  peptide (wild type A $\beta$ ). We monitor the effect of SDS on the aggregation of the A $\beta$  peptide at different D/P ratios. The ratios cover the entire range of SDS concentrations and were chosen to overlap with those employed by Wahlström et al. <sup>[20]</sup>. The present study shows that by EPR information about A $\beta$  aggregation at a wide range of SDS concentrations can be obtained. We propose that A $\beta$  aggregates, present in the absence of SDS, are successively replaced by peptide-detergent aggregates at low SDS concentrations. At SDS concentrations above the CMC only one species is present, which we assign to a monomeric, micelle bound form of A $\beta$ .

## **2.2 Materials and methods**

The A $\beta$ 40 peptide and its cysteine-A $\beta$  variant (H-Cys-Asp-Ala-...-Val-OH) were purchased from AnaSpec (purity > 95 %), the solvent DMSO was purchased from Biosolve (purity 99.8 %). The MTS spin label ((1-oxyl-2,2,5,5-tetramethylpyrrolidine-3-methyl) methanethiosulfonate) was purchased from Toronto Research Chemicals Inc. (Brisbane Rd., North York, Ontario, Canada, M3J 2J8). Spin labeling was performed and the purified spin-labeled A $\beta$  was analyzed by liquid chromatography as described previously <sup>[38]</sup>. The peptide was lyophilized and stored in the freezer (-20<sup>0</sup>C) until used.

### **2.2.1 Sample preparation protocol**

Seven different A $\beta$  sample conditions, differing in SDS concentrations were investigated. The total concentration of peptide was kept constant at 0.55 mM. The peptide was a mixture of wild type A $\beta$  and SL-A $\beta$  that contained 14 % SL-A $\beta$ , resulting in diamagnetically diluted samples as reported before <sup>[38]</sup>. In contrast to the previous protocol <sup>[38]</sup>, we prepared the A $\beta$  samples using a procedure, which involves predissolution of the peptide in dilute base solution <sup>[20,40-42]</sup>. This procedure was designed to avoid peptide aggregation in the starting solution.

Accordingly, the A $\beta$  peptides were predissolved in NaOH solution (10 mM, pH 11) with sonication for one minute in an ice bath at twice the desired final concentration, i.e., at 1.1 mM total A $\beta$  concentration. The desired amount of SDS was dissolved in potassium phosphate buffer (20 mM, pH 7.4). The basic solution of A $\beta$  peptides (1.1 mM) was combined with the potassium phosphate buffer solution (20 mM, pH 7.4) to reach the final desired peptide concentration and the proper D/P molar ratio for each sample (for D/P ratios see table 2.1). This step was followed by another one minute sonication in an ice bath. The final pH was adjusted to pH 7.4. The entire sample preparation was performed on ice. All samples were prepared and measured at least twice.

**Table 2.1** Correspondence of SDS content of samples. Ratio of SDS detergent to A $\beta$  peptide (D/P) and absolute SDS concentrations investigated.

D/P ratio	SDS [mM]
0	0
2.7	1.5
5.4	3
7.3	4
12.7	7
65.4	36
130.9	72

### 2.2.2 EPR experiments

For room temperature measurements, samples of 10-15  $\mu$ l peptide solution were drawn into Blaubrand 50  $\mu$ l capillaries. Often, a white precipitate was observed, indicating aggregation. In cases where a white precipitate was observed, the sample height was carefully adjusted in order to be sensitive to that part of the solution. The X-band continuous-wave (cw) EPR measurements have been performed using an ELEXSYS E680 spectrometer (Bruker, Rheinstetten, Germany) equipped with a rectangular cavity. A modulation frequency of 100 kHz was used. Measurements were done at temperature of 20°C, using 6.331 mW of microwave power and a modulation amplitude of 1.4 G. The large modulation amplitude helps to obtain a better signal-to-noise ratio for broad lines. The accumulation time for the spectra was 40 minutes per spectrum.

### 2.2.3 The amount of spin label in different samples

For a quantitative comparison of samples, we need to investigate the actual amount of spin label in each sample. This amount was determined by double integration of the first-derivative EPR spectrum, with the SL-A $\beta$  stock solution as a reference. The amount of spin label for the samples with different concentrations of SDS was at least 86 % compared to the stock solution. The uncertainties of this method, determined by multiple independent analyses of the same data, are around 20 % due to difficulties with the base-line correction of the spectra. Within this error margin, the amount of spin-labeled peptides in all samples is identical.

### 2.2.4 Simulations of EPR spectra, interpretation of the rotation-correlation time

The spectra were simulated using Matlab (version 7.11.0.584, Natick, Massachusetts, U.S.A) and the EasySpin package<sup>[43]</sup>. The following tensor values were used for all simulations:  $g = [2.00906, 2.00687, 2.00300]$ <sup>[38,44]</sup> and  $A_{xx} = A_{yy} = 13$  MHz in

buffer. For the fast and medium components, different  $A_{zz}$  values were used than for the slow component, as discussed before <sup>[38]</sup>. For each fraction over-modulation effects were taken into account in EasySpin. Usually a superposition of one to three components was required to simulate the spectra. In all cases, isotropic rotation of the spin label was sufficient to reproduce the line-shape observed. From the simulation of the EPR line-shape, the rotation-correlation time,  $\tau_r$ , of the spin-labeled peptide as well as the corresponding amount of each spectral component was obtained <sup>[45]</sup>.

We interpreted  $\tau_r$  with the Stokes-Einstein equation, which implies a spherical approximation for the volume <sup>[38]</sup>:

$$\tau_r = \frac{4\pi\eta\alpha^3}{3kT} = \frac{\eta}{kT} V_{EPR} \quad (2.1)$$

The Boltzman constant,  $k$ , and solvent viscosity,  $\eta$ , at a specified temperature,  $T$ , are required to obtain the hydrodynamic radius,  $\alpha$ . According to equation (2.1), the volume,  $V_{EPR}$ , of the particle is linearly correlated with the  $\tau_r$  of the spin-labeled peptide. The volumes derived are referred to as  $V_{EPR}$  in the text. The volume  $V_{EPR}$  derived from  $\tau_r$  is strongly affected by the mobility of the nitroxide group of the spin label and the rotation of the spin label around the linker bond can make this correlation time significantly smaller than that of the aggregate.

### 2.3 Results

We have applied X-band cw EPR to monitor the effects of the presence of SDS on the A $\beta$  peptide. The main observable is the line-shape of the EPR spectra, which, under the conditions employed (diamagnetic dilution), reflects the mobility of the spin label attached to the cysteine variant of A $\beta$ . Figure 2.1 shows the spectra of the monomeric SL-A $\beta$  and of diamagnetically diluted SL-A $\beta$  in three samples with different amounts of SDS measured at room temperature. In the following we refer to the diamagnetically diluted SL-A $\beta$  as SL-A $\beta$  unless otherwise stated.

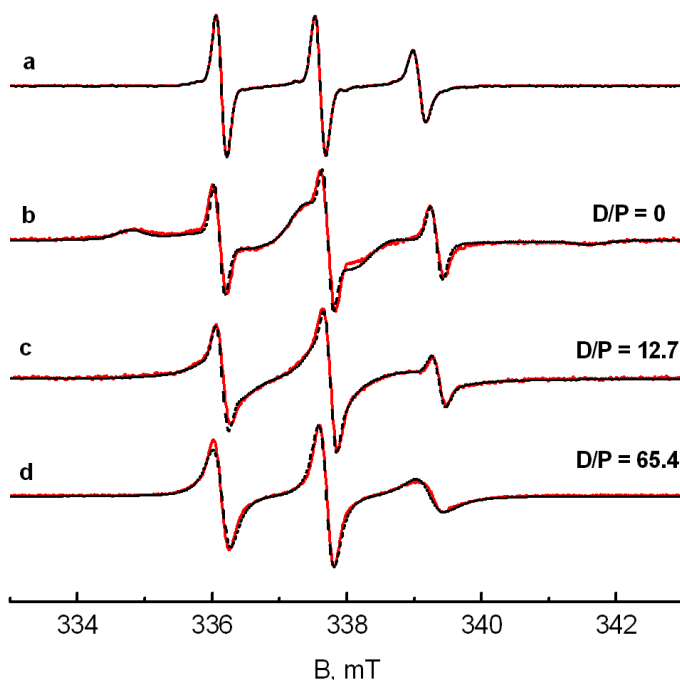


**Figure 2.1** Room temperature EPR spectra of monomeric pure SL-A $\beta$  in a: DMSO, and SL-A $\beta$  obtained from samples with three different D/P ratios: b: D/P = 0, c: D/P = 12.7 and, d: D/P = 65.4. Black line: experiment, red line: simulation.

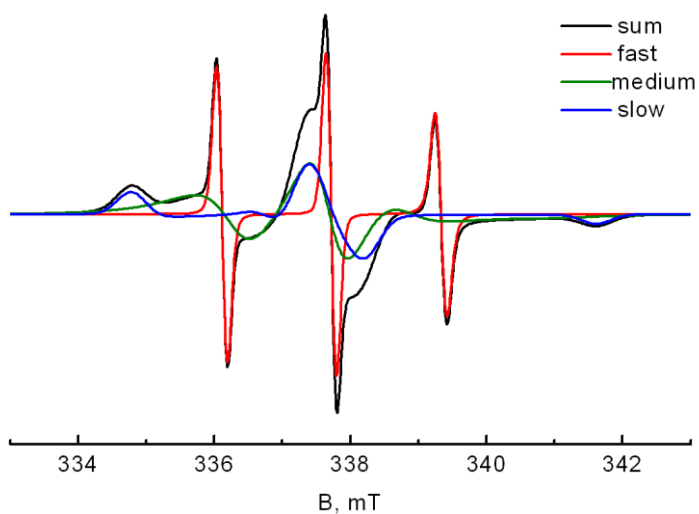


**Figure 2.2** Simulation of the EPR spectrum of SL-A $\beta$  at D/P = 0 with three components: red line fast, green line medium, and blue line slow component.



The EPR spectrum of monomeric A $\beta$  (figure 2.1.a) has three narrow lines. Comparison of figure 2.1.a and b shows that in the absence of SDS (D/P = 0), the lines are broadened and additional lines are observed compared to the spectra of the monomeric peptide (figure 2.1.a), which suggests a superposition of different spectral components. Figure 2.2 shows these components as obtained from a simulation of the EPR spectrum that is shown in figure 2.1.b. The spectrum can be simulated by three components<sup>[38]</sup>, which, in the remainder of the text, we refer to as fast, medium and slow. The relative amount of these components (table 2.2) is similar to that obtained before<sup>[38]</sup> except for an increase in the amount of the fast fraction from 5 % to 10 % (see Discussion). Each component is characterized by a rotation-correlation time and the amount by which this component contributes to the spectrum (table 2.2).

**Table 2.2** EPR parameters obtained from the simulation of cw EPR spectra of SL-A $\beta$  samples. Given are:  $\tau_r$ , rotation-correlation time,  $A_{zz}$ , the hyperfine splitting along the z-direction,  $lw$ , the component line-width of the simulation, and % stands for the contribution of the component to the total spectrum.

D/P	fast				medium				slow			
	$\tau_r$ (ns)	$A_{zz}$ (MHz)	$lw$ (mT)	%	$\tau_r$ (ns)	$A_{zz}$ (MHz)	$lw$ (mT)	%	$\tau_r$ (ns)	$A_{zz}$ (MHz)	$lw$ (mT)	%
0	0.19 ± 0.02	110	0.14	10 ± 2.0	2.55 ± 0.35	110	0.32	51 ± 2	> 50	95	0.50	39.0 ± 2.0
2.7	0.43 ± 0.02	110	0.14	2.5 ± 0.5	4.80 ± 0.40	110	0.32	64 ± 4	> 50	95	0.50	33.5 ± 2.5
5.4	0.43 ± 0.02	110	0.14	2.5 ± 0.5	4.65 ± 0.55	110	0.32	75 ± 3	> 50	95	0.50	22.5 ± 2.5
7.3	0.19 ± 0.02	110	0.14	10.0 ± 2.0	1.76 ± 0.16	110	0.14	90 ± 2	-	-	-	-
12.7	0.19 ± 0.02	110	0.14	7.0 ± 2.0	1.55 ± 0.08	110	0.14	92 ± 3	-	-	-	-
65.4	-	-	-	-	0.93 ± 0.03	109	0.06	100	-	-	-	-
130.9	-	-	-	-	0.93 ± 0.03	109	0.06	100	-	-	-	-

Figure 2.1.c shows the spectrum of a sample with an intermediate ratio of D/P (D/P = 12.7). This spectrum was simulated using two components (fast and medium) with the parameters given in table 2.2. The slow component disappears gradually in the range of SDS concentrations from 3 to 7 mM, D/P = 5.4 to 12.7. At even higher concentrations of SDS (above 36 mM, D/P = 65.4) the simulation shows that the line-shape (figure 2.1.d) is fully described by a single species. The corresponding  $\tau_r$  of this species is the same for the D/P ratios 65.4 and 130.9. The rotation-correlation time of the single species observed at high SDS concentrations ( $\tau_r = 0.93$  ns) is larger than the  $\tau_r$  of the fast component ( $\tau_r = 0.19$  ns) and smaller than that of

the medium component in the absence of SDS ( $D/P = 0$ ,  $\tau_r = 2.55$  ns). In the following we refer to this species as the high-SDS species.

To test for spin-spin interaction we measured the high-SDS species in a pure SL-A $\beta$  sample. The result is shown in figure 2.3. There is no difference between the diamagnetically diluted and the non-diluted sample, showing the absence of spin-spin interaction of A $\beta$  in the high SDS regime.

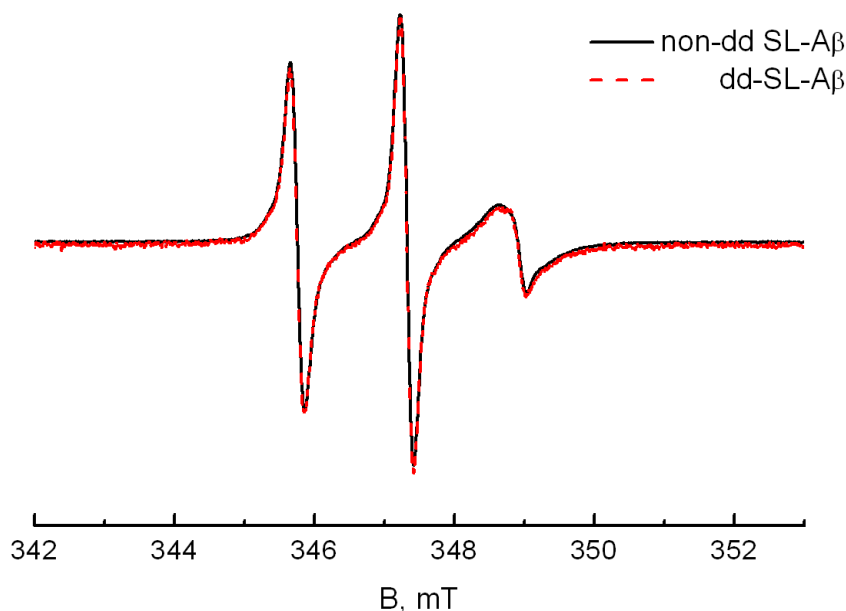


**Figure 2.3** Room temperature EPR spectra of high-SDS-A $\beta$  samples measured at a D/P ratio of 130.9. Black line: non-diluted A $\beta$  sample: non-dd SL-A $\beta$ . Red line: diamagnetically diluted A $\beta$  sample: dd-SL-A $\beta$ .

### 2.3.1 Effect of SDS on the amount of different components

An important parameter in the spectral simulation is the contribution of different components to each spectrum. In figure 2.4, the amount of different mobility components is plotted versus the D/P ratios ranging from 0 to 130.9. In the absence of SDS, at  $D/P = 0$ , the spectrum is composed of almost equal amounts of the slow and the medium component, and a small fraction (10 %) of the fast component. At low D/P ratios (between  $D/P = 0$  and 12.7), the amount of the fast component fluctuates but never reaches more than 12 %. At D/P ratios larger than 12.7 the fast component disappears. There is a gradual increase in the amount of the medium component between  $D/P = 0$  and 12.7. Above  $D/P = 12.7$  (i.e., 7 mM SDS) which is

close to the critical micelle concentration of SDS <sup>[22-25,27]</sup>, the medium component increases to its final value of 100 %. As shown in figure 2.4, upon increasing the D/P ratio to about D/P = 7.3, there is a drop in the amount of the slow component. At D/P ratios larger than 7.3 the slow component has disappeared.

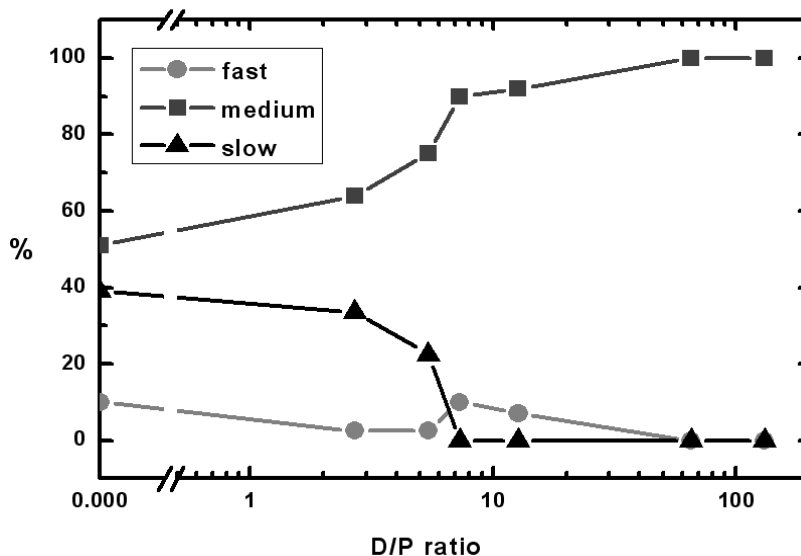


**Figure 2.4** Amount of the spectral components as a function of the D/P ratios.

### 2.3.2 The size of aggregates at different concentrations of SDS

According to the Stokes-Einstein equation, equation (2.1), the volume of the particle has a linear dependence on  $\tau_r$  (see materials and methods). From  $\tau_r$  we can determine the EPR derived volume of the aggregates,  $V_{EPR}$ , (see materials and methods). For the volume of the slow component ( $\tau_r > 50$  ns), only a lower limit of  $5 \cdot 10^4 \text{ \AA}^3$  could be given because this component is immobile on the time scale of the EPR experiment. For the fast rotating fraction of the sample with D/P = 0, a  $\tau_r$  of 0.19 ns is obtained. Using the viscosity of water of  $\eta = 1.002 \cdot 10^{-3} \text{ (N}\cdot\text{s}\cdot\text{m}^{-2})$  at 20° C <sup>[46]</sup>, a volume of  $180 \text{ \AA}^3$  results, which is close to the volume of  $126 \text{ \AA}^3$  obtained from the  $\tau_r$  of A $\beta$  in DMSO ( $\eta = 1.996 \cdot 10^{-3} \text{ N}\cdot\text{s}\cdot\text{m}^{-2}$  <sup>[46]</sup>,  $\tau_r = 0.26$  ns) in which the peptide is in the monomeric form. Following Sepkhanova et al., the fast component is assigned to the monomeric peptide <sup>[38]</sup>.

## 2.4 Discussion

In the present study we have used spin-label EPR to investigate the effect of SDS on the aggregation process of the A $\beta$  peptide. In the absence of SDS, three components are found, which, according to their mobility characteristics, are referred to as the fast, medium, and slow components. We attribute the fast component to monomeric A $\beta$  and the two others to aggregated forms of A $\beta$ , as described before<sup>[38]</sup>. We ascribe the larger amount of monomeric A $\beta$  (10 % vs 5 % in the previous study) observed in the present study to the different preparation protocol<sup>[20,40,42]</sup>, a protocol that was designed to increase the amount of monomeric A $\beta$ . The fraction of monomeric A $\beta$  never reaches values higher than 12 %, even considering the sample-to-sample variation. From this observation, we conclude that the largest portion of the sample is aggregated. This observation is in good agreement with previous reports<sup>[10,20]</sup>, which shows that at the A $\beta$  concentrations used here aggregates are present.

### 2.4.1 The high SDS concentration species of A $\beta$

At high concentrations of SDS, well above CMC<sup>[22-27]</sup>, the sample is composed of a single species, referred to as the high-SDS-species. This species makes up at least 80 % of the total peptide in the sample (see materials and methods) and is the only species we observe. In that state, the A $\beta$  must be monomeric because of the absence of spin-spin interaction in the spectra of pure SL-A $\beta$  samples (figure 2.3 and appendix A). This species has a molecular volume  $V_{\text{EPR}}$  that is larger than the  $V_{\text{EPR}}$  of the monomeric A $\beta$ . The  $V_{\text{EPR}}$  of the high-SDS species is much smaller than the volume of an SDS micelle<sup>[22,47]</sup>. Previously, it was proposed that the species predominant at high SDS concentrations is a monomeric A $\beta$ , solubilized in an SDS micelle<sup>[17,20,28,29,31,32,34,48]</sup>. This proposal is consistent with the data obtained by EPR. The finding that the size of the high-SDS species is larger than that of the monomeric A $\beta$  is consistent with micelle binding, because the volume increases by the attachment of A $\beta$  to the micelle. The fact that  $V_{\text{EPR}}$  is smaller than the volume of the SDS micelle is attributed to the local mobility of the spin label. Also, owing to the local mobility of the spin label,  $V_{\text{EPR}}$  is significantly smaller than the volume of the high-SDS species ( $23 - 132 \cdot 10^3 \text{ \AA}^3$ ) derived from NMR results<sup>[20,32,34,48]</sup>. The last issue to be resolved for the high-SDS species is that EPR suggests the sample to be homogenous, whereas the NMR-titration data show that at similar D/P ratios, the sample is heterogeneous, and only a fraction of about 20 % of the sample is visible to the NMR, which shows that only that fraction is in the monomeric SDS-micelle bound form<sup>[20]</sup>. Several explanations are offered for the absence of NMR signals for the remaining 80 % of the peptide, amongst which peptide aggregates<sup>[20]</sup>. For

the EPR sample we can exclude a mixture of aggregates and monomers because only a single species is observed and  $A\beta$ - $A\beta$  interaction is not detected (figure 2.3 and appendix A). Besides other explanations given for the heterogeneity of the high-SDS NMR samples <sup>[20]</sup>, differences between the EPR and NMR results could be caused by the respective measurement conditions. It has been shown that the absolute concentrations of SDS and  $A\beta$  could influence the formation of the  $A\beta$ -micelle complex or peptide aggregation, because apparently there is competition between the association of  $A\beta$  with micelles and  $A\beta$  with  $A\beta$  to form aggregated peptide <sup>[17]</sup>. The peptide concentration in the EPR experiments is higher than in NMR. Consequently, the critical micelle concentration of SDS is reached at lower D/P ratios than in the NMR experiments. This could help to favorably influence the equilibrium between  $A\beta$ - $A\beta$  and  $A\beta$ -SDS interaction and result in a larger fraction of monomeric  $A\beta$  bound to the micelle in the EPR experiment. Furthermore, in the EPR sample preparation the total amount of SDS is added directly to the peptide, rather than in titrating steps as in NMR <sup>[20]</sup>. Perhaps the presence of high concentrations of SDS under the conditions of the EPR measurement is more efficient to prevent peptide aggregation.

#### 2.4.2 $A\beta$ at intermediate SDS concentrations

In contrast to the interpretation of the high-SDS-species, much less is known so far about the state of peptide at intermediate concentrations of SDS. The disappearance of NMR signals and the  $\beta$ -sheet signatures found in CD and FTIR spectra were attributed to an aggregated form of  $A\beta$  <sup>[20]</sup>. By EPR, in the intermediate SDS concentration regime (D/P = 2.7),  $\tau_r$  of the medium component (table 2.2) is larger than in the absence of SDS, which could be due to an increase in the size of existing aggregates or to detergent molecules that bind to  $A\beta$ . In the former case, such aggregates are most likely formed at the expense of the very large aggregates present in the slow mobility fraction. Such a redistribution would explain the decreasing amount of  $A\beta$  in the slow fraction with increasing SDS concentration, a fraction that at D/P ratios of 7.3, corresponding to 4 mM SDS, completely disappears. But concomitantly, also the character of the aggregate must change, as also suggested by the decrease in the  $\beta$ -sheet component observed by CD spectroscopy <sup>[20]</sup>. The rotation-correlation time of the medium-mobility fraction changes significantly at D/P ratios between 7.3 and 12.7 to 1/3 of its initial value, which indicates a change in the size of the aggregate and/or the local mobility of the spin label. We speculate that the aggregate changes from an  $A\beta$ -oligomer to a species in which  $A\beta$  interacts with several SDS molecules. The component observed is likely not the micelle bound species, because the transition occurs well

below the CMC of SDS. Almost coinciding with the CMC, at D/P ratios above 12.7 the high-SDS species prevails.

Overall, the present EPR investigation suggests that, starting from low SDS concentrations, a transition from an A $\beta$ -oligomer to an A $\beta$ -SDS complex seems to take place. Since this change is accompanied by a loss in  $\beta$ -sheet signature and an increase in  $\alpha$ -helix character <sup>[20]</sup>, we propose that this is the first step towards the micelle-bound state of A $\beta$ , in which the peptide is supposed to have an  $\alpha$ -helical structure.

The present investigation shows that because of the high sensitivity of EPR to the aggregation state of A $\beta$ , we can monitor the changes occurring in the reaction mixture in the presence of different amounts of SDS on the time scale of aggregation. We propose an A $\beta$ -SDS complex at SDS concentrations below the CMC and a micelle-bound monomeric A $\beta$  state at higher SDS concentrations.

Reference List

- [1] F.Chiti, C.M.Dobson, *Annu.Rev.Biochem.* **2006**, 75 333-366.
- [2] D.G.Lynn, S.C.Meredith, *J.Struct.Biol.* **2000**, 130 153-173.
- [3] M.Margittai, R.Langen, *Q.Rev.Biophys.* **2008**, 41 265-297.
- [4] F.Panza, V.Solfrizzi, V.Frisardi, C.Capurso, A.D'Introno, A.M.Colacicco, G.Vendemiale, A.Capurso, B.P.Imbimbo, *Drugs Aging* **2009**, 26 537-555.
- [5] D.J.Selkoe, *Neuron* **1991**, 6 487-498.
- [6] D.J.Selkoe, *Physiol Rev.* **2001**, 81 741-766.
- [7] M.Gralle, S.T.Ferreira, *Prog.Neurobiol.* **2007**, 82 11-32.
- [8] J.Hardy, D.J.Selkoe, *Science* **2002**, 297 353-356.
- [9] S.Kumar, S.K.Mohanty, J.B.Udgaonkar, *J.Mol.Biol.* **2007**, 367 1186-1204.
- [10] A.Paivio, J.Jarvet, A.Gräslund, L.Lannfelt, A.Westlind-Danielsson, *Journal of Molecular Biology* **2004**, 339 145-159.
- [11] C.J.Barrow, M.G.Zagorski, *Science* **1991**, 253 179-182.
- [12] P.Cizas, R.Budvytyte, R.Morkuniene, R.Moldovan, M.Brocchio, M.Losche, G.Niaura, G.Valincius, V.Borutaite, *Arch.Biochem.Biophys.* **2010**, 496 84-92.
- [13] F.Dulin, I.Callebaut, N.Colloc'h, J.P.Mornon, *Biopolymers* **2007**, 85 422-437.
- [14] N.L.Fawzi, J.F.Ying, D.A.Torchia, G.M.Clore, *Journal of the American Chemical Society* **2010**, 132 9948-9951.
- [15] D.Losic, L.L.Martini, M.I.Aguilar, D.H.Small, *Biopolymers* **2006**, 84 519-526.
- [16] D.J.Tew, S.P.Bottomley, D.P.Smith, G.D.Ciccotosto, J.Babon, M.G.Hinds, C.L.Masters, R.Cappai, K.J.Barnham, *Biophysical Journal* **2008**, 94 2752-2766.
- [17] J.M.Lin, T.L.Lin, U.S.Jeng, Z.H.Huang, Y.S.Huang, *Soft Matter* **2009**, 5 3913-3919.
- [18] B.ONuallain, D.B.Freir, A.J.Nicoll, E.Risse, N.Ferguson, C.E.Herron, J.Collinge, D.M.Walsh, *J.Neurosci.* **2010**, 30 14411-14419.
- [19] V.Rangachari, B.D.Moore, D.K.Reed, L.K.Sonoda, A.W.Bridges, E.Conboy, D.Hartigan, T.L.Rosenberry, *Biochemistry* **2007**, 46 12451-12462.
- [20] A.Wahlström, L.Hugonin, A.Perálvarez-Marín, J.Jarvet, A.Gräslund, *FEBS J.* **2008**, 275 5117-5128.
- [21] S.S.S.Wang, K.N.Liu, T.C.Han, *Biochimica et Biophysica Acta-Molecular Basis of Disease* **2010**, 1802 519-530.
- [22] G.Duplatre, M.F.F.Marques, M.daGracaMiguel, *Journal of Physical Chemistry* **1996**, 100 16608-16612.
- [23] E.Fuguet, C.Rafols, M.Roses, E.Bosch, *Analytica Chimica Acta* **2005**, 548 95-100.
- [24] A.Helenius, K.Simons, *Biochim.Biophys.Acta* **1975**, 415 29-79.
- [25] G.D.Henry, B.D.Sykes, *Nuclear Magnetic Resonance, Pt C* **1994**, 239 515-535.
- [26] P.Mukerjee, K.J.Mysels, P.Kapauan, *Journal of Physical Chemistry* **1967**, 71 4166-&.
- [27] M.Sammalkorpi, M.Karttunen, M.Haataja, *J.Phys.Chem.B* **2007**, 111 11722-11733.
- [28] J.Jarvet, J.Danielsson, P.Damberg, M.Oleszczuk, A.Gräslund, *J.Biomol.NMR* **2007**, 39 63-72.
- [29] M.Coles, W.Bicknell, A.A.Watson, D.P.Fairlie, D.J.Craik, *Biochemistry* **1998**, 37 11064-11077.
- [30] T.A.Pertinhez, M.Bouchard, R.A.Smith, C.M.Dobson, L.J.Smith, *FEBS Lett.* **2002**, 529 193-197.
- [31] V.Rangachari, D.K.Reed, B.D.Moore, T.L.Rosenberry, *Biochemistry* **2006**, 45 8639-8648.
- [32] H.Y.Shao, S.C.Jao, K.Ma, M.G.Zagorski, *Journal of Molecular Biology* **1999**, 285 755-773.
- [33] D.V.Waterhous, W.C.Johnson, Jr., *Biochemistry* **1994**, 33 2121-2128.
- [34] M.G.Zagorski, L.M.Hou, *Abstracts of Papers of the American Chemical Society* **2002**, 223 C29.
- [35] M.Grimaldi, M.Scrima, C.Esposito, G.Vitiello, A.Ramunno, V.Limongelli, G.D'Errico, E.Novellino, A.M.D'Ursi, *Biochim.Biophys.Acta* **2010**, 1798 660-671.
- [36] F.Mito, T.Yamasaki, Y.Ito, M.Yamato, H.Mino, H.Sadasue, C.Shirahama, K.Sakai, H.Utsumi, K.Yamada, *Chemical Communications* **2011**, 47 5070-5072.
- [37] G.Vitiello, M.Grimaldi, A.Ramunno, O.Ortona, G.De Martino, A.M.D'Ursi, G.D'Errico, *Journal of Peptide Science* **2010**, 16 115-122.

- [38] I.Sepkhanova, M.Drescher, N.J.Meeuwenoord, R.W.A.L.Limpens, R.I.Koning, D.V.Filippov, M.Huber, *Applied Magnetic Resonance* **2009**, 36 209-222.
- [39] F.Scarpelli, M.Drescher, T.Rutters-Meijneke, A.Holt, D.T.Rijkers, J.A.Killian, M.Huber, *J.Phys.Chem.B* **2009**, 113 12257-12264.
- [40] Y.Fezoui, D.M.Hartley, J.D.Harper, R.Khurana, D.M.Walsh, M.M.Condron, D.J.Selkoe, P.T.Lansbury, Jr., A.L.Fink, D.B.Teplow, *Amyloid* **2000**, 7 166-178.
- [41] Y.Fezoui, D.M.Hartley, D.M.Walsh, D.J.Selkoe, J.J.Osterhout, D.B.Teplow, *Nat.Struct.Biol.* **2000**, 7 1095-1099.
- [42] L.Hou, H.Shao, Y.Zhang, H.Li, N.K.Menon, E.B.Neuhaus, J.M.Brewer, I.J.Byeon, D.G.Ray, M.P.Vitek, T.Iwashita, R.A.Makula, A.B.Przybyla, M.G.Zagorski, *J.Am.Chem.Soc.* **2004**, 126 1992-2005.
- [43] S.Stoll, A.Schweiger, *Journal of Magnetic Resonance* **2006**, 178 42-55.
- [44] S.Steigmiller, M.Börsch, P.Gräber, M.Huber, *Biochim.Biophys.Acta* **2005**, 1708 143-153.
- [45] W.L.Hubbell, H.S.Mchaourab, C.Altenbach, M.A.Lietzow, *Structure* **1996**, 4 779-783.
- [46] L.M.Omoto, O.Iulian, O.Ciocirlan, I.Nita, *Revue Roumaine de Chimie* **2008**, 53 977-+.
- [47] F.Bockstahl, E.Pachoud, G.Duplatre, I.Billard, *Chemical Physics* **2000**, 256 307-313.
- [48] H.Y.Shao, S.C.Jao, M.G.Zagorski, *Abstracts of Papers of the American Chemical Society* **1997**, 213 13-MEDI.